energies

MDPI

Article

Independent Control of Active and Reactive Power Flow for a Single-Phase, Unidirectional Onboard Power Converter Connecting the DC Power Bus to the AC Bus

Tomasz Binkowski [1,*] and Paweł Szcześniak [2]

[1] Faculty of Electrical and Computer Engineering, Rzeszow University of Technology, Al. Powstańców Warszawy 12, 35-959 Rzeszów, Poland

[2] Institute of Automatic Control, Electronics and Electrical Engineering, University of Zielona Góra, 65-516 Zielona Góra, Poland; p.szczesniak@iee.uz.zgora.pl

* Correspondence: tbinkow@prz.edu.pl

Abstract: The paper presents a proposed system that supplies a 400 Hz single-phase onboard grid from the DC onboard bus. This system enables independent compensation of reactive power in the AC grid. Independent control of active and reactive power flow requires the decomposition of current in the grid into active and reactive components. Independent control of active and reactive power requires the use of synchronizers that operate in the *dq* frame system. If synchronization is performed with a single-phase grid, the transformation of *dq* requires the virtual quadrature signals. Standard quadrature signal generation systems use a second-order generalized integrator. To improve the dynamics of the system, the paper proposes a new quadrature generator that operates on the basis of trigonometric calculations instead of a second-order integration system. The developed system was implemented in a proportional-resonant current control system. Tests carried out in steady state and in dynamic states related to typical grid disturbances proved significantly better dynamic properties than those of a standard integrator-based system.

Keywords: power transfer; compensator; P+R controller; quadrature signal generator

Citation: Binkowski, T.; Szcześniak, P. Independent Control of Active and Reactive Power Flow for a Single-Phase, Unidirectional Onboard Power Converter Connecting the DC Power Bus to the AC Bus. *Energies* **2024**, *17*, 540. https://doi.org/10.3390/en17020540

Academic Editor: Fabio Immovilli

Received: 20 November 2023
Revised: 18 January 2024
Accepted: 20 January 2024
Published: 22 January 2024

1. Introduction

With the development of power electronic converters, electronic devices and apparatuses are replacing traditional mechanical and pneumatic systems. The simplicity of power control and elimination of mechanical couplings are advantages that characterize more electric applications used in industry and households, as well as on ships, aircraft, and space vehicles [1]. Particularly important is the application of electric devices onboard vehicles, where the weight and size of the devices are critical. With the use of electrical devices, it is possible to reduce the size of the device operating at the same power. This result is obtained by increasing the frequency of the supply voltages. Consequently, this requires the application of energy converters that precisely control the power of electrical machines.

The onboard power management system integrates a number of power buses with different parameters. Typical buses found in onboard electrical systems include DC and AC buses. To effectively manage energy on board a mobile platform, it is often necessary to flow power to various loads on a continuous or temporary basis. This is especially important when there are high-power loads on board that are characterized by pulsating operation. Power transmission is performed using grid converters, which are being studied by many researchers [2,3]. The use of a grid converter connecting a DC bus to a single-phase AC grid causes a number of problems. One of them is the occurrence of power ripples with double grid frequency. The problem of its elimination has been studied in many research centers and presented in many articles. From this work, it is concluded that one of two approaches can be used to attenuate or eliminate power ripple. The first approach uses a converter with an additional active circuit. The second approach is characterized by modifying the control method by implementing techniques to change the voltage or current waveform [4,5]. When active circuits are applied, ripple is suppressed by additional passive components due to capacitive or inductive energy storage capability. Power decoupling techniques based on the implementation of an additional circuit can be implemented as a series or parallel circuit on the AC, DC, or AC side, as described in [4]. The size and volume of additional inductive-capacitive resonant elements used in the auxiliary circuit would be very large due to the relatively low resonant frequency, which greatly limits the application area [5–7], especially in an onboard system. When the bulky electrolytic capacitor or auxiliary active or resonant circuit is limited, the effect of the second harmonic current in a single-phase converter can be reduced by properly implementing the control method [8].

The main objectives of the power flow control system of the grid inverter include control of the active power and synchronization with the grid voltages. If the inverter is not loaded with rated power, its reserve can be used to compensate for the reactive power. It results in a reduction in the RMS value of the current in the AC grid, thereby reducing energy losses on the AC buses. With decoupled power control, it is possible to achieve a relatively stable output voltage on the DC bus during disturbances. The most commonly used power control decoupling techniques can be divided into passive decoupling [9,10] and active decoupling [11–13]. Although the first one is simple to implement, its applications in the aerospace industry are not desirable due to the requirement for large capacitors. Active power decoupling control, on the other hand, is more promising. In the case of DC/DC converters connecting energy storage and the DC bus, the voltage fluctuation range of the decoupling capacitor can be increased. In the end, the capacitor used for power decoupling can be very small, and the power on the DC bus can be significantly increased. There are two commonly used control strategies for active decoupling, which are serial decoupling [14] and parallel decoupling [15]. Although serial decoupling has higher conversion efficiency, it requires two DC/DC conversion stages. It increases costs and reduces reliability. At the same time, the parallel decoupling strategy is widely used in real-world applications. This is due to the use of only a bidirectional DC/DC converter and the support of the power conversion process through the use of batteries. Estimating the state of health of the battery presented in the works [16,17] allows for the design of an economic system that helps increase the specific power of the system.

For three-phase AC systems, a phase-locked loop (PLL) system based on a *dq* frame is best for controlling active and reactive power [18,19]. In an unbalanced three-phase grid system, the negative sequence of the dual fundamental frequency can affect the accuracy of the PLL. They then used the low-pass-filtered negative sequence of the AC component and the DC component of the positive sequence for grid phase locking. The authors of [20] and [21] constructed a new circuit to generate the positive AC component. They then used it for phase locking, improving the speed and accuracy of the phase synchronization loop. The PLL's performance is affected by power quality parameters such as frequency stepping, amplitude, and phase angle fluctuations, as well as the presence of harmonic distortion. It follows that the PLL should operate effectively in a disturbed grid condition [22].

For synchronization with a single-phase grid, many synchronization techniques with good performance known from three-phase systems cannot be used. In single-phase grids, techniques based on Enhanced PLL (EPLL) [23] and Second-Order Generalized Integrator (SOGI-PLL) [24] are mostly applied. To improve the dynamics and accuracy of the PLL and to reduce the computational burden, the paper proposes a quadrature generator to replace the SOGI system in a PLL. The use of a quadrature signal generator, which is simple in digital implementation, eliminates the second-order integral system, replacing it with trigonometric equations. The equations have a form with only the cosine function. This function, stored in a look-up table, makes it easy to access its values for the system. It improves the dynamics of the whole system. The proposed system based on trigonometric formulas (TFB-PLL) was used in a single-phase system for current decoupling. As a result, it is possible to independently set the reference current values corresponding to the active power and the reactive power generated by the inverter. The ability to set the reactive component of the current unlocked the possibility of operating the inverter in reactive power compensator mode.

The rest of the article is organized as follows. Section 2 presents the system using the proposed TFB-PLL synchronization technique. The block structure of the onboard buses is shown together with the location of the inverter. The quadrature generator concept is described in detail, and the mathematical equations of the quadrature signals are derived. Based on these equations, the generator was constructed, and the general form of the PLL system that uses it was shown. The concept of controlling decoupled current components based on proportional-resonant control is also presented. Section 3 presents the tuning procedure of the proposed PLL system and the results of steady state and dynamic tests of the phase synchronization loop. Selected waveforms of the modified onboard system are also shown. Section 4 presents the final conclusions.

2. Materials and Methods

The study deals with the control system of energy flow in an onboard power system containing a DC bus and an AC bus. This paper focuses primarily on the control of a power electronic converter with a role of unidirectional energy transfer from the DC bus to the AC bus in a way that allows simultaneous and independent control of the active and reactive components of the current, enabling simultaneous control of the active power transferred to the AC bus and the reactive power. Controlling the active power allows the supply of the required power to the loads connected to the AC bus while reducing the load of the AC generators. This situation is particularly important when the pulsed equipment on board is powered by the AC bus. Reactive power control allows the use of DC power sources to compensate for reactive power on the AC bus. The volume of transferred active power is determined by its availability on the DC bus and limited by the rating parameters of the power electronic converter. The value of the reactive components of the current is limited not only by the ratings of the converter currents but also by the value of the active component of the current fed into the AC bus.

Research on the control system was carried out on an existing onboard system, which includes a grid converter with an H-bridge structure as the inverter. This inverter connects the DC bus to the onboard AC system at 400 Hz. An overview system showing the structure studied consisting of AC and DC buses, a grid converter, and a control system is shown in Figure 1. The tasks of the grid converter control system include managing active power and reactive power, which is achieved by controlling the active and reactive components of the current that feeds the onboard AC grid. The implementation of this control task requires the use of a modulator circuit that outputs a set current from the grid. This current must have the parameters required to achieve the set values of active and reactive power. These parameters are controlled in a controller system with proportional resonant characteristics. The structure of such a controller, which has better implementation characteristics due to the limited gain, is described in detail in [25].

Control of active and reactive components of the power supplied to the AC grid requires a specific system of synchronization with its voltage. Determining the reference value of active and reactive power requires the operation of multiplying the reference value of the active and reactive components of the grid converter current by a sine and cosine signal corresponding to the fundamental component of the voltage, respectively. Signals must hold their shape independent of measurement noise and distortion components in the grid voltage. In three-phase systems, synchronization with the grid voltage is achieved by controlling the xy frame using the Clark and Park transforms. The system under consideration is a single-phase system, so the Clark transformation cannot be applied. For synchronization, rather than the SOGI system, the paper proposes a system that was developed based on trigonometric formulas. Assuming that the single-phase onboard grid is sinusoidal, the following voltage is described by the formula:

$$v_g = V_g \cos\omega t, \tag{1}$$

where v_g is the voltage waveform of the onboard AC grid, V_g is the voltage amplitude, and ω is the angular frequency of the grid. The transition to orthogonal components requires synchronization of the angle θ of the xy frame with the voltage vector of the grid defined by the components v_α and v_β. The relations between the angles are shown in Figure 2.

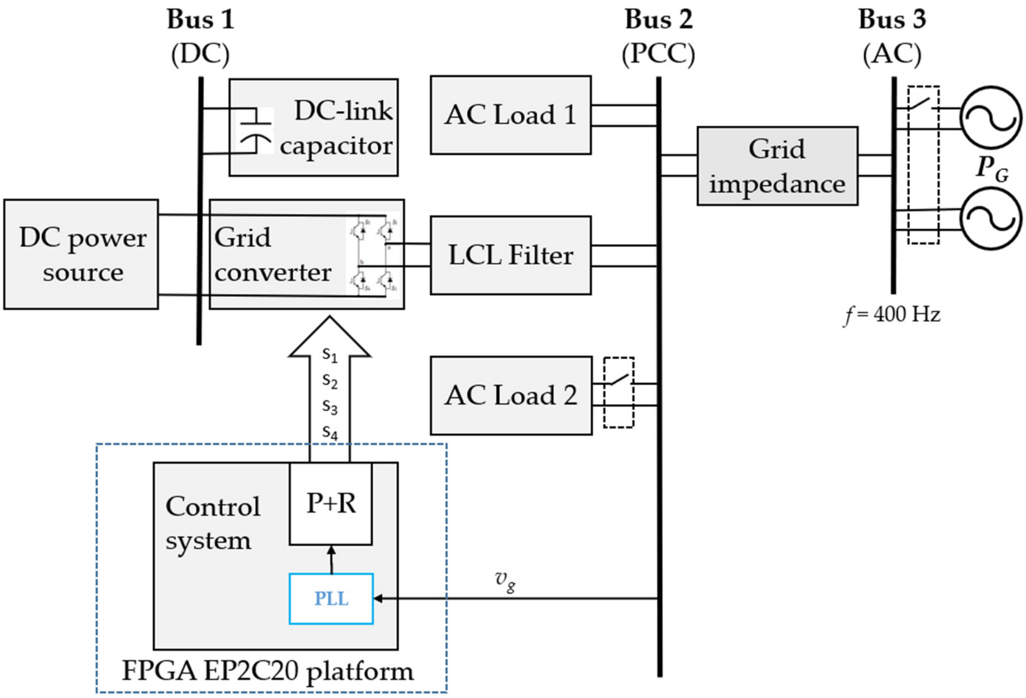

Figure 1. Diagram of the onboard power distribution system.

Figure 2 shows that the virtual grid voltage vector $\vec{V}_g$ with orthogonal components v_α and v_β can be expressed as:

$$\vec{V}_g = v_\alpha + \mathrm{j}\, v_\beta = \mathrm{V}_g \cos\omega t + \mathrm{j}\, \mathrm{V}_g \sin\omega t. \tag{2}$$

In the fully synchronized steady state of the system, the virtual voltage vector of the grid has the same phase angle as the xy frame, consequently satisfying the conditions:

$$\begin{cases} \theta = \omega t \\ v_d = V_g \\ v_q = 0 \end{cases}. \tag{3}$$

Then, the grid voltage vector can be expressed as:

$$\begin{cases} v_\alpha = V_g \cos\omega t = v_d \cos\theta \\ v_\beta = V_g \sin\omega t = v_d \sin\theta \end{cases}. \tag{4}$$

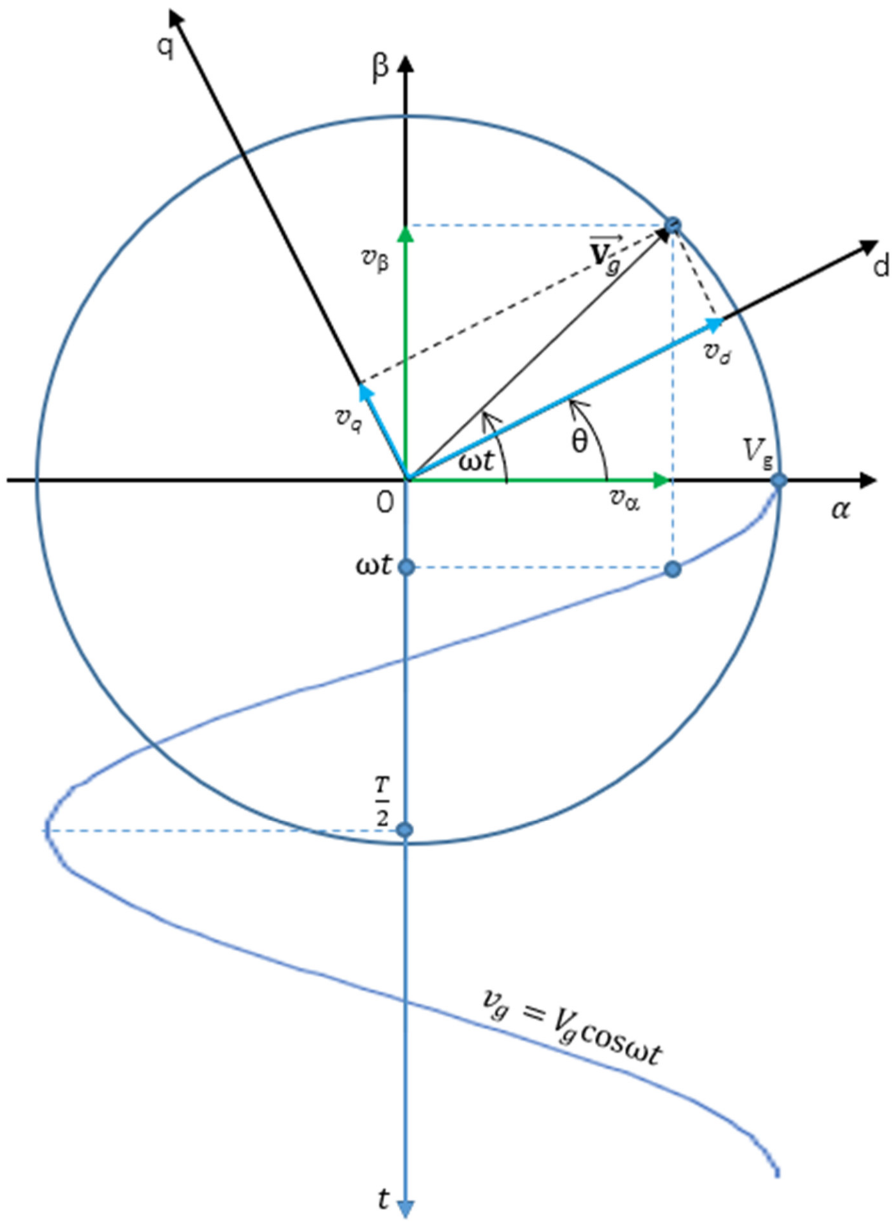

Figure 2. Graphical interpretation of orthogonal signal generation.

Applying the well-known trigonometric formulas:

$$2\sin x\cos x = \sin 2x, \tag{5}$$

$$2\cos^2 x - 1 = \cos 2x, \tag{6}$$

and assuming $x = \theta/2$, Equation (4) can be expressed as follows:

$$\begin{cases} v_\alpha = V_g\cos\theta = 2V_g\cos^2\frac{\theta}{2} - V_g \\ v_\beta = V_g\sin\theta = 2\,V_g\sin\frac{\theta}{2}\cos\frac{\theta}{2} \end{cases}. \tag{7}$$

As mentioned, the system of Equation (7) is correct only in the steady state when the condition given by Equation (3) is satisfied. Substituting the angle $\theta/2$ for the angle ωt in the equation describing v_β, the following general form of quadrature signals is obtained:

$$\begin{cases} v_\alpha = V_g\left(2\cos^2\frac{\theta}{2} - 1\right) \\ v_\beta = 2V_g \sin\omega t \cos\frac{\theta}{2} \end{cases}. \tag{8}$$

Equation (8) shows that the voltage of the single-phase onboard grid is used to synchronize the xy frame with the voltage vector only through the v_β component. The result is a computationally simplified system that replaces the SOGI structure. The proposed system formulates a quadrature signal system (QSS) in block form, as shown in Figure 3.

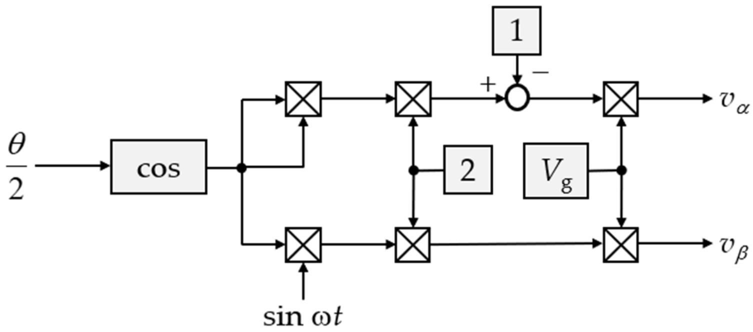

Figure 3. Block structure of the quadrature signal generator.

Based on the proposed equations for establishing the orthogonal components, it is possible to use the conventional PLL structure operating in the dq rotating system. The proposed PLL structure based on trigonometric formulas (TFB-PLL) is shown in Figure 4.

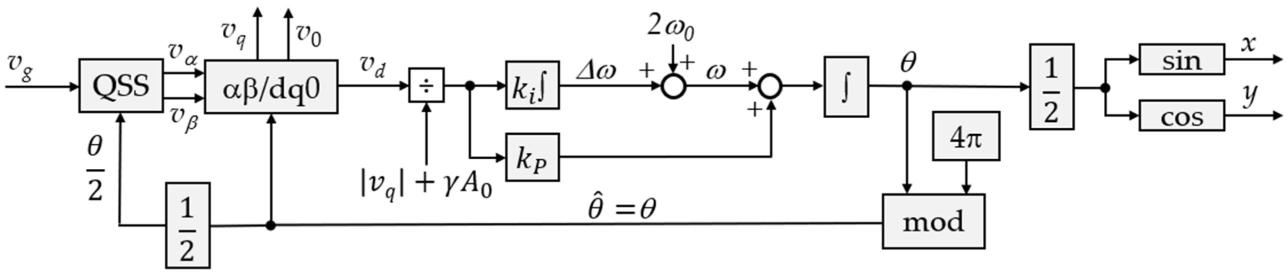

Figure 4. Block diagram of the single-phase PLL with proposed QSS, where: input signal (v_g), orthogonal components (v_α and v_β), dq0-axis components of the input (v_d, v_q and v_0), rated frequency of the input (ω_0), unitary output signal synchronous with the input (x), delayed unitary output signal (y), estimated angle (θ), estimated frequency (ω), proportional gain (k_P) and integrating gain (k_i).

The orthogonal components calculated from the trigonometric formulas are transformed into the dq system, excluding the zero component, according to the relation:

$$\begin{bmatrix} V_d \\ V_q \end{bmatrix} = \begin{bmatrix} \cos\theta & \sin\theta \\ -\sin\theta & \cos\theta \end{bmatrix} \begin{bmatrix} V_g\cos\theta \\ V_g\sin\theta \end{bmatrix} = V_g \begin{bmatrix} \cos(\omega t - \theta) \\ \sin(\omega t - \theta) \end{bmatrix}. \tag{9}$$

When the PI control system reaches steady state, the components of dq can be expressed as (10).

$$\begin{bmatrix} V_d \\ V_q \end{bmatrix} = V_g \begin{bmatrix} 1 \\ 0 \end{bmatrix}. \tag{10}$$

Based on the proposed synchronization rules, when Equation (10) is satisfied, control of the active and reactive components of the bus current can be carried out based on the components v_α and v_β. The components v_α and v_β calculated in the proposed PLL system are used to determine the deviation of the AC bus current e_g relative to the reference current i_{ref} according to the expression:

$$e_g = i_{ref} - i_g = i_{aref}\cos\omega t + i_{rref}\sin\omega t - i_g, \tag{11}$$

where i_g is the measured current of the AC bus, i_{aref} and i_{rref} are the active and reactive reference components of the grid current, respectively. The determined value of the deviation e_g is the input signal of the proportional-resonant control system with limited gain, described by transmittance shown as (12).

$$\mathrm{H}(s) = k\frac{s^2 + \left(\frac{1}{Tk} + \frac{k_R}{T}\right)s + \left(\frac{1}{T^2}\right)}{s^2 + \left(\frac{k_R}{T}\right)s + \left(\frac{1}{T^2}\right)}, \tag{12}$$

where T is the internal integration constant of the resonant part, and k and k_R are the gains of the proportional and resonant parts, respectively.

Figure 5 shows a block diagram of the converter control system. Control of the active and reactive power supplied to the grid is based on the difference between the current of the grid and the reference value of this current. The grid current reference value is calculated from the reference value of the active and reactive components of the grid current and the quadrature signals x and y synchronous with the grid voltage. The quadrature signals are generated by the proposed TFB-PLL system. This system, replacing the standard second-order generalized integrator with trigonometric formulas, reduces the time required to achieve the state of synchronization of the controller with the grid voltage.

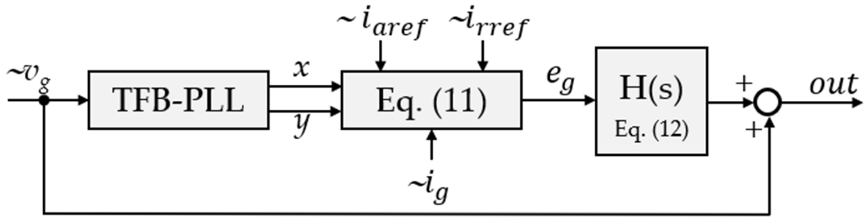

Figure 5. Block diagram of the proposed control system with the TFB-PLL.

3. Results

The experiments were conducted in two categories to evaluate the performance of the proposed system in steady state and dynamic states. Hardware in the Loop (HIL) experiments allow us to evaluate the TFB-PLL system itself, while hardware tests allow us to evaluate the control system with the FFB-PLL system implemented. The HIL tests carried out are designed to verify the adopted concept of generating quadrature signals and observe the PLL response to typical perturbations of AC grid voltage parameters such as frequency, phase angle, and amplitude. The group of HIL tests also includes tests to evaluate the comparative dynamics of the proposed TFB-PLL system with the standard SOGI system, as well as experiments to observe the behavior of the TFB-PLL under harmonically distorted voltage. The second group of experiments concerns the study of the converter control system in which the proposed TFB-PLL system is implemented. These experiments are designed to evaluate how the improved PLL system affects the control system. The tests of this group concern hardware tests and refer to the observation of waveforms for changes in reference signals and changes in AC-grid voltage parameters.

The system proposed in the paper for controlling the active and reactive components of the converter's current was tested in an onboard power system that used a single-phase grid inverter. This inverter transferred energy from the DC bus to the 400 Hz AC bus. The main and primary task of the inverter is to supply energy to the onboard AC system from DC power sources. As an improvement on standard control structures, a system is proposed that has the functionality of a reactive power compensator in addition to energy transfer. The system described in Section 2 was implemented in digital form in an Altera FPGA reconfigurable device of EP2C20 type.

The parameters of the TFB-PLL system shown in Figure 4 were adjusted according to the standard procedure. Information on the rated magnitude of A_0 was used only to avoid a possible division by zero in the division block. This block was added to make the parameter settings depend on the amplitude of the input signal. The γ constant was assumed to be 0.001. The natural frequency ω_n = 0.25ω_0 = 628 rad/sec and a reasonable value of the damping ratio ξ = 0.7 was adopted for a good trade-off between transient time and filtering strength. Based on the assumed coefficients, the TFB-PLL gains were calculated as follows:

$$k_P = 2\xi\omega_n = 879 \tag{13}$$

$$k_i = \omega_n^2 = 394384 \tag{14}$$

By analyzing the transient time of TFB-PLL, it can be shown that the time constant of the system response is around one full cycle of 400 Hz:

$$\tau = \frac{1}{\xi\omega_n} \approx 2.3\ \text{ms} < \frac{1}{f}. \tag{15}$$

To limit the range of frequency oscillations caused by a phase angle step change or during the start-up process, an adaptive integral gain k_i was added, which can be calculated based on Equation (16).

$$k_i = \omega_n^2 \frac{1}{1 + \rho \frac{|v_d|}{|v_q| + \gamma A_0}} \tag{16}$$

In the tests carried out, the adaptive function was disabled by taking ρ = 0. Assuming a nonzero value would reduce false fluctuations in frequency estimation caused by phase-step change at the cost of reducing the actual speed of frequency estimation, and this would limit the formulation of comparative conclusions.

The system was carried out in two directions. In the first path, tests were performed on the TFB-PLL system implemented in an FPGA as a hardware-in-the-loop (HIL) system. The PLL system was run as a system running in parallel with systems that emulate input signals. The second path involved testing using a hardware setup. The investigation conducted in both paths refers to testing in the steady state and transient.

3.1. HIL Tests

To evaluate the proposed quadrature generator, tests were performed on the HIL system. A digital PLL system was first started and tested by observing the steady-state PLL response. The result of the recorded waveform of the input signal v_g and the orthogonal components v_α and v_β are shown in Figure 6a. The registration results obtained confirm the assumptions regarding the generation of orthogonal signals, where the correct phase shift and overlap of the v_α component signal with the input signal are shown. In the next stage of the study, dynamic tests were performed, in which the PLL system's responses to step changes in input signal parameters were recorded. To estimate the PLL response time t_r, the value of the root square error (17) was used from the difference in the instantaneous value of the signal at the PLL's input and output.

$$e(t) = \left(v_g(t) - v_\alpha(t)\right)^2 \tag{17}$$

The system was tested by recording the PLL response to a frequency step change from 400 to 401 Hz, a phase angle step change of pi/4, and a 40% amplitude step change. The results obtained for the PLL input and output are shown in Figure 6b–d, respectively.

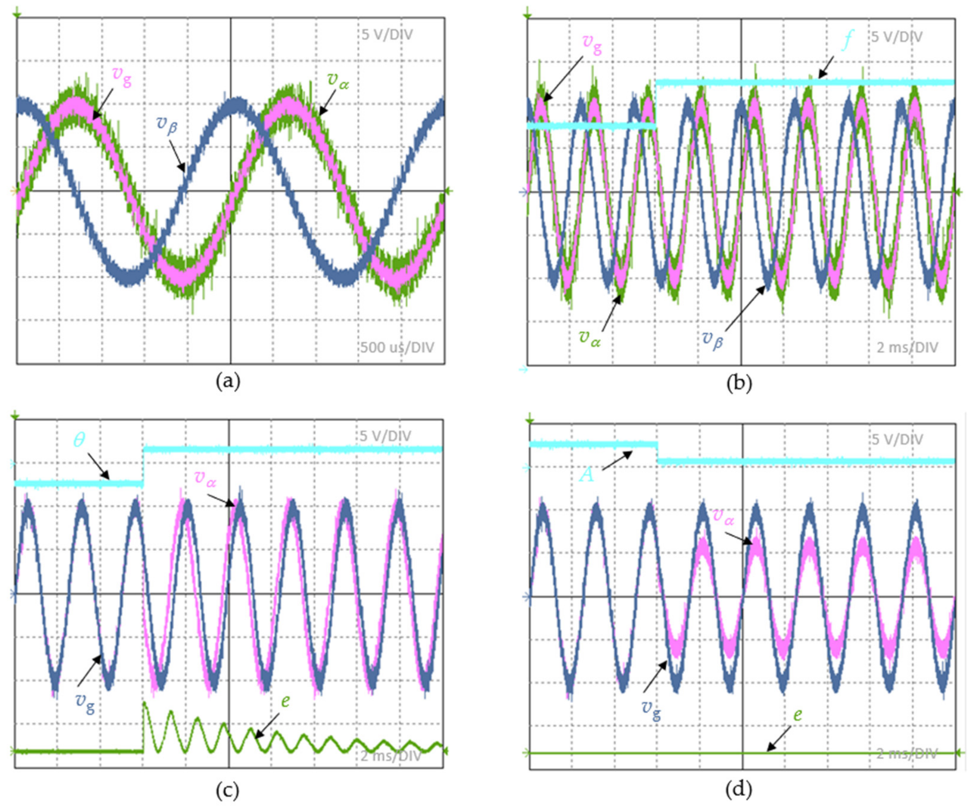

Figure 6. Signals of the proposed TFB-PLL: (**a**) waveforms of the input signal v_g and orthogonal response signals v_α and v_β in steady state; (**b**) waveforms of the input signal v_g, orthogonal response signals v_α and v_β and frequency f during the frequency step change; (**c**) waveforms of the input signal v_g, response signal v_α, phase angle θ, and error e during the phase angle step change; (**d**) waveforms of the input signal v_g, response signal v_α, amplitude A and error e during the amplitude step change.

In the experiment, for comparison, it was assumed that the criterion determining the response time of the PLL t_r is measured until the signal e reaches a value of 0.01. Using such a criterion, response time measurements were made for step changes in the phase shift angle theta and for step changes in the frequency Δf. The results obtained are shown in Figure 7, from which it can be concluded that for a step change in the phase shift angle less than 30 degrees and for frequency step change less than 30 hertz, TFB-PLL establishes steady state in less than two milliseconds. This is in accordance with the design assumptions implied by Formula (15).

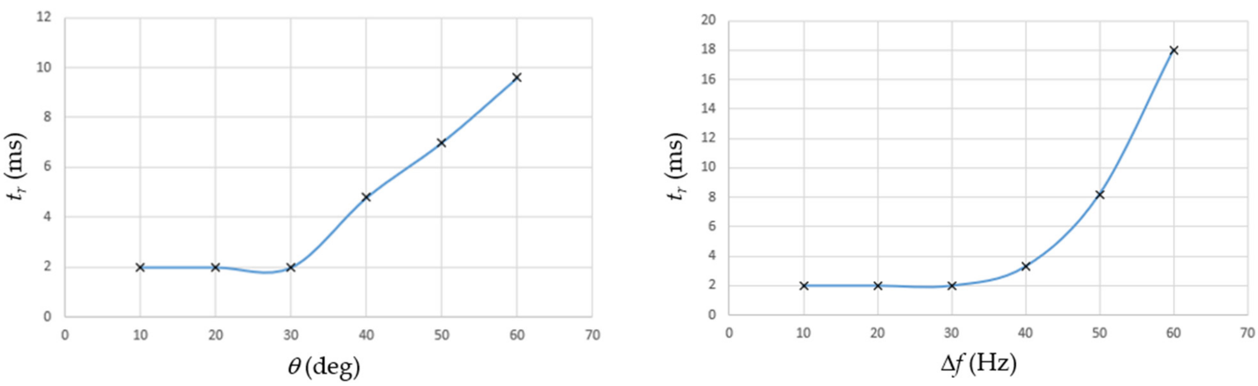

Figure 7. TFB-PLL response times as a function of the phase angle step change value and the frequency step change value.

In addition to observing the behavior of the input and output of the PLL in steady state and with a step change in the input parameters, the waveforms of the d and q components inside the PLL system and the waveform of the squared error, calculated according to Formula (17), were recorded in analogous cases. A summary of the results obtained is shown in Figure 8.

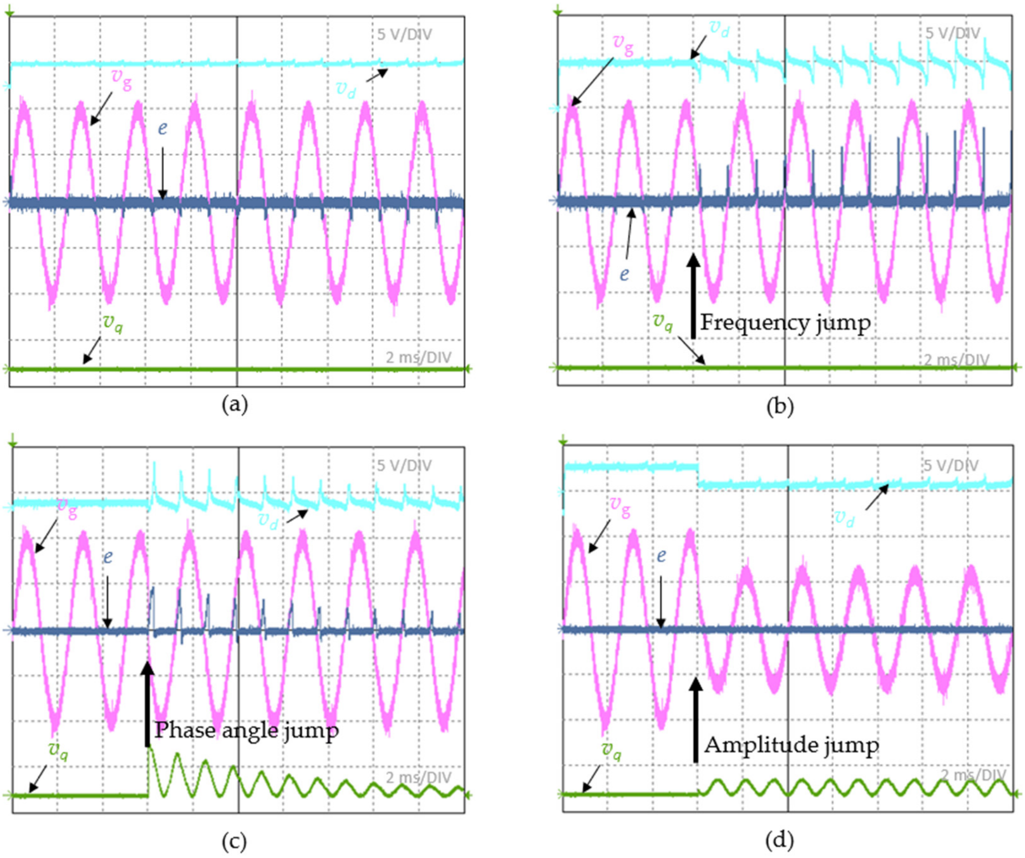

Figure 8. Signals of the proposed TFB-PLL: (**a**) waveforms of the input signal v_g, response *dq* signals v_d, v_q, and error signal *e* in steady state; (**b**) waveforms of the input signal v_g, response *dq* signals v_d, v_q, and error signal *e* during the frequency step change; (**c**) waveforms of the input signal v_g, response *dq* signals v_d, v_q, and error signal *e* during the phase angle step change; (**d**) waveforms of the input signal v_g, response *dq* signals v_d, v_q and error signal *e* during the amplitude step change.

PLL system tests were also performed for an input signal that contains the third harmonic of the fundamental component A_o with an amplitude of 20%. For the cases involving the testing of step changes in the parameters of the input signal, recording of the input and output waveforms was performed along with the waveform of the e signal. The results are shown in Figure 9a. The oscillograms of the components *dq*, along with the waveform of the input signal and the signal e, are shown in Figure 9b.

From the analysis of the waveforms obtained, it can be clearly seen that the proposed concept of a quadrature generator in a PLL system based on the *dq* transformation meets the basic requirements and is a good alternative to other well-known quadrature systems. However, to expose the advantages of the proposed system, a comparative analysis was carried out. In this analysis, analogous tests of a quadrature system with a SOGI structure were performed, and the quadrature signals for the two systems under comparison were recorded in a parallel manner. Figure 10a shows the waveforms of the orthogonal components v_α and v_β during the start of the PLL loop for the variant with the proposed generator and for the SOGI generator. Since the proposed system is based on trigonometric formulas, it does not show the existence of significant transient components in this case. For the SOGI system, the transient is clearly shown and is about five periods of the input signal.

In the case of a step change in frequency from 400 to 401 Hz, the waveforms obtained are shown in Figure 10b. In this case, the influence of the SOGI integrator system is also clearly shown in the form of significant values of the transient component appearing. Against the signals of the SOGI system, the transient in the proposed system is not noticeable. The same conclusions can be reached by observing the output signals of the proposed system and the SOGI-based system for a step change in phase angle by π/4 and for a step change in amplitude to 60%, as shown in Figure 10c,d, respectively.

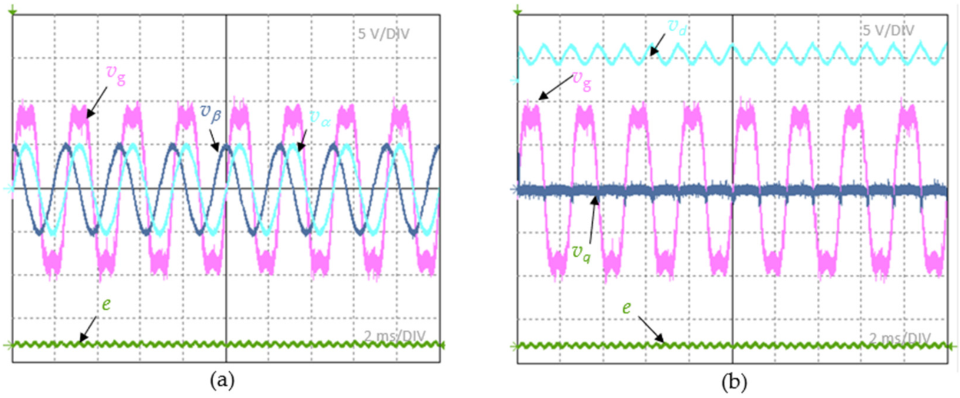

Figure 9. Signals of the proposed TFB-PLL for third harmonic: (**a**) waveforms of the input signal v_g, orthogonal response signals v_α and v_β and error signal e (**b**) waveforms of the input signal v_g, response dq signals vd, vq, and error signal e.

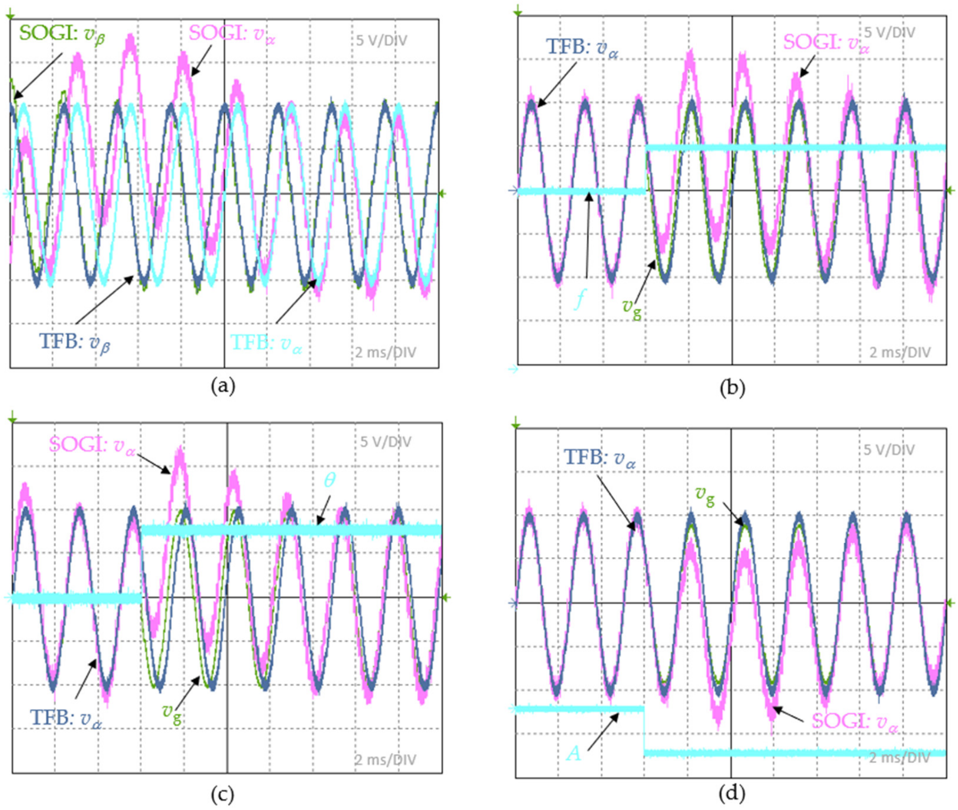

Figure 10. Comparison of orthogonal waveforms for (**a**) the SOGI system and the proposed TFB system in steady state; (**b**) the SOGI system and the proposed TFB system for the frequency step change; (**c**) the SOGI system and the proposed TFB system for the phase angle step change; (**d**) the SOGI system and the proposed TFB system for the amplitude step change.

The performed tests of the PLL system implemented in the FPGA, which included tests in steady state and transients caused by step changes in the parameters of the input signal, allow us to conclude that the TFB system proposed in the paper can be used as a good equivalent to standard quadrature generators. This is further confirmed by a comparative analysis of the results obtained for the SOGI system.

3.2. Hardware Setup Tests

Successful testing of the TMB-PLL system in the HIL system allowed a further experiment to be carried out. This experiment focused on testing the onboard system shown in Figure 11. In the same FPGA structure, the current proportional-resonant control processes and the inverter modulator were implemented.

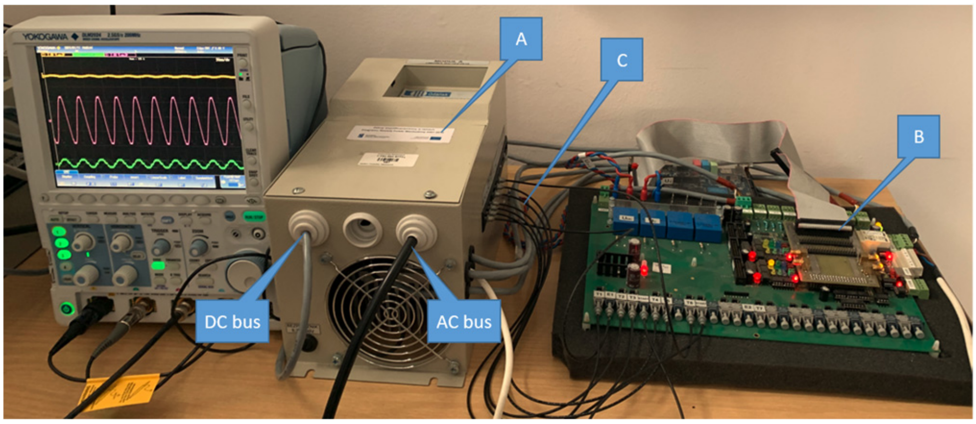

Figure 11. Laboratory bench: A—grid-connected converter, B—onboard control board with FPGA, C—fiber optic couplers.

Since the control system allows for independent control of the active and reactive components of the current, it was run with the TMB-PLL system proposed in the paper. The experiment was planned in such a way that the current and voltage waveforms of the grid were recorded for a dynamic state consisting of a step change in the reference value of the active component of the current with zero reactive component, a static state for the same values of the active and reactive reference components, a dynamic state corresponding to a constant active component of the current and the appearance of an inductive reactive component, and a dynamic state corresponding to the task of a step change in the reactive component of the current with a constant reference value of the active component. The case where the active component changes from 4 to 8 A in the absence of the reactive component is shown in Figure 12a. The recorded current is in phase with the voltage, indicating that the inverter is in the mode of injecting energy from the DC source into the 400 Hz onboard grid. Figure 12b shows the current and voltage of the grid in the static state when the inverter is set in the additive reactive power compensation mode of the grid. The set values for the reference active component and the reference inductive reactive component are 4 A. In this case, the current waveform should be 45 electrical degrees ahead of the voltage waveform, which is confirmed by the oscillogram shown. The case of operation with a step forcing of the reference inductive and capacitive reactive component of 4 A with a reference active component of 4 A is shown in Figure 12c,d, respectively. The appearance of an inductive and capacitive angle shift of 45 degrees is shown in the included oscillograms. Figure 12 also confirms the rule of graphical orthogonal vector folding, where for non-zero active and reactive components, the amplitude of the grid current increases.

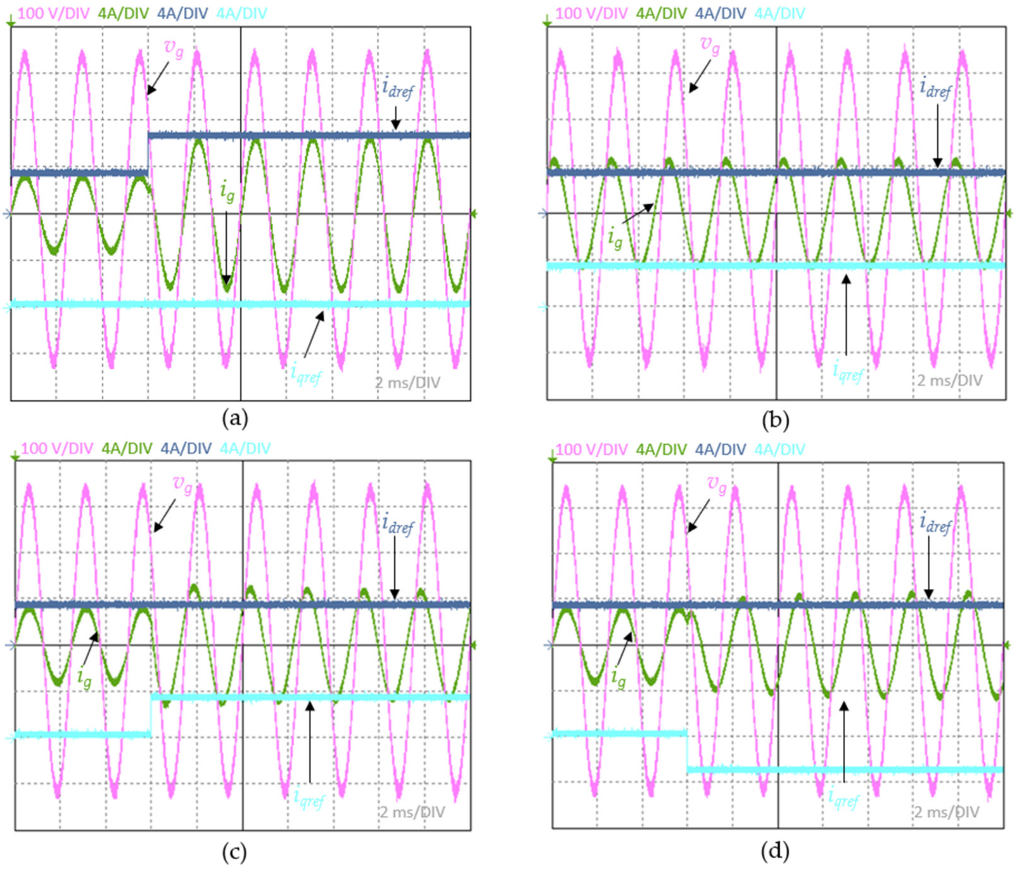

Figure 12. Waveforms of the grid voltage v_g, grid current i_g, referenced active component i_{dref}, referenced reactive component i_{qref} of the onboard system for: (**a**) zero reactive component and active component step change from 4 to 8 A; (**b**) 4A reactive and active component; (**c**) step change from 0 to 4A inductive reactive component and 4A active component; (**d**) step change from 0 to 4A capacitive reactive component and 4A active component.

After experimentally verifying the current and voltage waveforms relating to the reconstruction of the reference values of the active and reactive components of the current, steps in the grid voltage parameters, the case of a drop in the grid voltage to 80% of the nominal value of the amplitude and a step change in the phase angle in the grid voltage by an angle of $\pi/4$ was recorded. In the case shown in Figure 13a, as a result of the decrease in the voltage of the grid, there is a step change in the active component of the voltage with a zero reactive component. This is due to the fact that the analyzed case referred to a compensated grid. From the lack of change in the amplitude of the grid current, it can be deduced that the control system is feeding energy into the grid at a preset level, undisturbed by the voltage drop. A step change in the phase angle of the grid voltage results in the appearance of disturbances in the recorded v_d and v_q signals in TFB-PLL. These disturbances are reduced as the control system becomes synchronous with the grid voltage. The current at such a disturbance does not show changes that would allow us to conclude that the basic function of the converter, i.e., feeding energy into the grid at a set level, has been disturbed. This case is illustrated in Figure 13b.

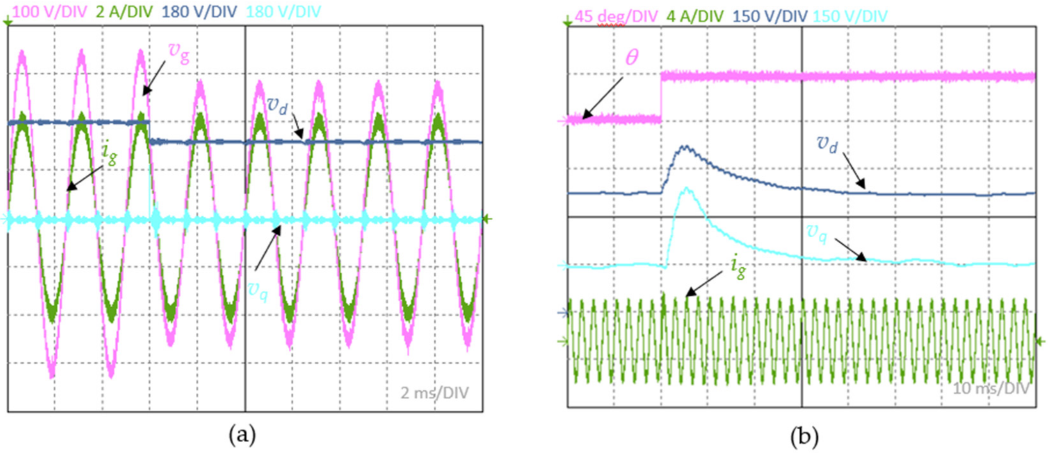

Figure 13. Waveforms of the grid voltage v_g, grid current i_g, and dq components i_d, i_q of the onboard system for (**a**) 10% voltage drop; (**b**) phase angle step change.

The disturbance in the flow of energy to the grid is most affected by the change in frequency of the grid voltage. This disturbance is affected not only by the dynamics of the PLL system but also by the dynamics of the control system and delays in the measurement tract. Figure 14 shows the response observed in the amplitude of the grid current, which resulted from a 1% step change in frequency. A clear reduction in the current amplitude is shown after the disturbance occurred, which was suppressed after about 50 ms. Taking into account the results presented in Section 3.1, it can be concluded that this is the effect of the control system connecting with its resonant frequency. Taking into account the fact that this type of disturbance generally does not occur in onboard grids, and if it does occur, it is in a transient manner, where the frequency returns to its rated value after a short time, this problem was considered to be of little importance.

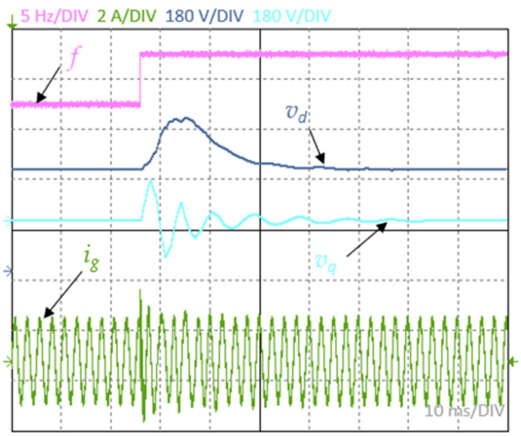

Figure 14. Waveforms of the grid current i_g and dq components i_d, i_q of the onboard system for the frequency step change.

The experiments of the proposed TFB-PLL show that simple calculations based on trigonometric formulas can be used to generate the quadrature signals required for a PLL system based on the dq transformation. It allows us to replace the second-order generalized integration system with a system characterized by easy implementation, reduced over-regulation, and reduced PLL response time. The application of the proposed system in the control system of a single-phase grid converter allows independent control of active and reactive power in a more efficient way by shortening dynamic processes and ensuring stable operation.

4. Conclusions

The method proposed in this paper for generating quadrature signals necessary for synchronization with the grid of the proportional-resonant control system is characterized by shorter response times than other methods used in PLL systems. Due to the fact that calculations are performed on trigonometric formulas, the dynamics of TFB-PLL are better than those of the most commonly used SOGI-PLL system. Allowing synchronization with a single-phase *dq* onboard grid makes the grid current decouple into active and reactive components. Due to such decoupling of current components, the underloaded to rated values inverter can be used as a compensator for reactive power appearing in the onboard grid. Experiments show that a system with very good dynamics, which meets the requirements formulated at the beginning, has been obtained. In further work on the system, studies are planned to adapt the system's parameters to improve dynamics even more. Tests of adaptive integral gain and adaptation of natural frequency values in the proportional-integral controller PLL are planned, as well as implementation of TFB-PLL in other onboard devices operating with the 400 Hz AC grid.

Author Contributions: Conceptualization, T.B.; methodology, T.B.; software, T.B.; validation, T.B. and P.S.; formal analysis, T.B.; investigation, T.B.; resources, T.B. and P.S.; data curation, T.B. and P.S.; writing—original draft preparation, T.B.; writing—review and editing, T.B. and P.S.; visualization, T.B.; supervision, T.B.; project administration, T.B.; funding acquisition, T.B. and P.S. All authors have read and agreed to the published version of the manuscript.

Funding: This research was funded by the Minister of Education and Science of the Republic of Poland within the "Regional Initiative of Excellence" program for years 2019–2023. Project number 027/RID/2018/19. The APC was funded by private funds.

Institutional Review Board Statement: Not applicable.

Informed Consent Statement: Not applicable.

Data Availability Statement: Data are contained within the article.

Conflicts of Interest: The authors declare no conflict of interest.

References

1. Parripati, M.; Devi, V. A Single Phase DC-AC Inverter for Aircraft Application. In Proceedings of the Fourth International Conference on Inventive Systems and Control (ICISC), Coimbatore, India, 8–10 January 2020; pp. 250–255.
2. Kjær, S.; Pedersen, J.; Blaabjerg, F. A Review of Single-Phase Grid-Connected Inverters for Photovoltaic Modules. *IEEE Trans. Ind. Appl.* **2005**, *41*, 1292–1306. [CrossRef]
3. Tang, Y.; Blaabjerg, F. Power decoupling techniques for single-phase power electronics systems—An overview. In Proceedings of the 2015 IEEE Energy Conversion Congress and Exposition (ECCE), Montreal, QC, Canada, 20–24 September 2015; pp. 2541–2548.
4. Vitorino, M.; Alves, L.; Wang, R.; Correa, M. Low-Frequency Power Decoupling in Single-Phase Applications: A Comprehensive Overview. *IEEE Trans. Power Electron.* **2017**, *32*, 4. [CrossRef]
5. Zhang, L.; Ruan, X. Control Schemes for Reducing the Second Harmonic Current in Two-Stage Single-Phase Converter: An Overview from DC-Bus Port-Impedance Characteristic. *IEEE Trans. Power Electron.* **2019**, *34*, 10341–10358. [CrossRef]
6. Zhang, L.; Ruan, X.; Ren, X. Second Harmonic Current Reduction for Two-Stage Inverter with Boost-Derived Front-End Converter: Control Schemes and Design Considerations. *IEEE Trans. Power Electron.* **2017**, *33*, 6361–6378. [CrossRef]
7. Shi, Y.; Liu, B.; Duan, S. Low-Frequency Input Current Ripple Reduction Based on Load Current Feed-Forward in Two-Stage Single-Phase Inverter. *IEEE Trans. Power Electron.* **2015**, *31*, 7972–7985. [CrossRef]
8. Binkowski, T. A Conductance-Based MPPT Method with Reduced Impact of the Voltage Ripple for One-Phase Solar Powered Vehicle or Aircraft Systems. *Energies* **2020**, *13*, 1496. [CrossRef]
9. Crider, J.M.; Sudhoff, S.D. Reducing impact of pulsed power loads on microgrid power systems. *IEEE Trans. Smart Grid* **2010**, *1*, 270–277. [CrossRef]
10. Gu, Y.; Zhang, D.; Fang, M.; Zhang, X.; Qi, P. Research on low input current ripple two-stage converter for low frequency pulsed-power applications. *IET Power Electron.* **2020**, *13*, 340–345. [CrossRef]
11. Huang, X.; Ruan, X.; Du, F.; Fei, L.; Li, Z. A pulsed power supply adopting active capacitor converter for low-voltage and low-frequency pulsed loads. *IEEE Trans. Power Electron.* **2018**, *33*, 9219–9230. [CrossRef]
12. Yang, P.; Shang, Z.; Liu, C.; Peng, Y.; Zhu, Z. A three-state dual inductance bi-directional converter and its control in pulse-loaded three-port converters. *CSEE J. Power Energy Syst.* **2020**, *6*, 291–297.

13. Huang, X.; Ruan, X.; Du, F.; Fei, L.; Li, Z. High power and low voltage power supply for low frequency pulsed load. In Proceedings of the IEEE Applied Power Electronics Conference and Exposition, Tampa, FL, USA, 26–30 March 2017.
14. Yang, X.; Chen, P.; Chen, R.; Peng, Y.; Xu, J. Stability Improvement of Pulse Power Supply With Dual-Inductance Active Storage Unit Using Hysteresis Current Control. *IEEE J. Emerg. Sel. Top. Circuits Syst.* **2021**, *11*, 111–120. [CrossRef]
15. Xiao, W.; El Moursi, M.S.; Khan, O.; Infield, D. Review of grid-tied converter topologies used in photovoltaic systems. *IET Renew. Power Gener.* **2016**, *10*, 1543–1551. [CrossRef]
16. Gao, J.; Yang, D.; Wang, S.; Li, S.; Wang, L.; Wang, K. State of health estimation of lithium-ion batteries based on Mixers-bidirectional temporal convolutional neural network. *J. Energy Storage* **2023**, *73*, 109248. [CrossRef]
17. Liu, Y.; Wang, L.; Li, D.; Wang, K. State-of-health estimation of lithium-ion batteries based on electrochemical impedance spectroscopy: A review. *Prot. Control. Mod. Power Syst.* **2023**, *8*, 41. [CrossRef]
18. Subramanian, C.; Kanagaraj, R. Single-phase grid voltage attributes tracking for the control of grid power converters. *IEEE J. Emerg. Sel. Topics Power Electron.* **2014**, *2*, 1041–1048. [CrossRef]
19. Yan, Z.; He, H.; Li, J.; Su, M.; Zhang, C. Double fundamental frequency PLL with second order generalized integrator under unbalanced grid voltages. In Proceedings of the 2014 International Power Electronics and Application Conference and Exposition, Shanghai, China, 5–8 November 2014; pp. 108–113.
20. Guo, Z.; Zhang, Q.; Zhang, C.; Pang, J.; Yan, Z. A new method of double fundamental frequency phase-locked loop based on two integrators. In Proceedings of the 2016 Sixth International Conference on Instrumentation & Measurement, Computer, Communication and Control (IMCCC), Harbin, China, 21–23 July 2016; pp. 659–664.
21. Zheng, L.; Geng, H.; Yang, G. Fast and robust phase estimation algorithm for heavily distorted grid conditions. *IEEE Trans. Ind. Electron.* **2016**, *63*, 6845–6855. [CrossRef]
22. Golestan, S.; Guerrero, J.M.; Vasquez, J.C. Single-phase PLLs: A review of recent advances. *IEEE Trans. Power Electron.* **2017**, *32*, 9013–9030. [CrossRef]
23. Zhang, R.; Cardinal, M.; Szczesny, P.; Dame, M. A grid simulator with control of single-phase power converters in D-Q rotating frame. In Proceedings of the 2002 IEEE 33rd Annual IEEE Power Electronics Specialists Conference, Proceedings (Cat. No.02CH37289), Cairns, Australia, 23–27 June 2002; pp. 1431–1436.
24. Karimi-Ghartemani, M.; Karimi, H.; Khajehoddin, S.A.; Hoseinizadeh, S.M. Efficient modeling and systematic design of enhanced phase-locked loop structures. *IEEE Trans. Power Electron.* **2022**, *37*, 9061–9072. [CrossRef]
25. Nowak, M.; Binkowski, T.; Piróg, S. Proportional-Resonant Controller Structure with Finite Gain for Three-Phase Grid-Tied Converters. *Energies* **2021**, *14*, 6726. [CrossRef]